

Primitive Simultaneous Optimization of Similarity Metrics for Image Registration

Diana Waldmannstetter^{1,2*}, Florian Kofler^{1,3,4,5}, Benedikt Wiestler⁵, Julian Schwarting⁵, Ivan Ezhov^{1,4}, Marie Metz⁵, Daniel Rueckert^{6,7}, Jan S. Kirschke⁵, Marie Piraud³, and Bjoern H. Menze²

¹ Department of Informatics, Technical University of Munich, Munich, Germany

² Department of Quantitative Biomedicine, University of Zurich, Zurich, Switzerland

³ Helmholtz AI, Helmholtz Zentrum München, Munich, Germany

⁴ TranslaTUM - Central Institute for Translational Cancer Research, Technical University of Munich, Munich, Germany

⁵ Department of Diagnostic and Interventional Neuroradiology, School of Medicine, Klinikum rechts der Isar, Technical University of Munich, Munich, Germany

⁶ Artificial Intelligence in Healthcare and Medicine, Technical University of Munich, Munich, Germany

⁷ Department of Computing, Imperial College London, London, U.K.

Abstract. Even though simultaneous optimization of similarity metrics represents a standard procedure in the field of semantic segmentation, surprisingly, this does not hold true for image registration. To close this unexpected gap in the literature, we investigate in a complex multi-modal 3D setting whether simultaneous optimization of registration metrics, here implemented by means of primitive summation, can benefit image registration. We evaluate two challenging datasets containing collections of pre- to post-operative and pre- to intra-operative Magnetic Resonance Imaging (MRI) of glioma. Employing the proposed optimization we demonstrate improved registration accuracy in terms of Target Registration Error (TRE) on expert neuroradiologists' landmark annotations.

Keywords: Registration · Brain Tumor · Similarity Metric · Loss Function · Glioma

1 Introduction

Gross tumor resection represents the standard treatment for glioma. Clinicians measure the success of surgery by comparing pre- and post-operative scans. Furthermore, this comparison is required for subsequent treatment planning, such as radiation therapy. Image registration techniques can enhance this process by providing a direct overlay of the differing structures. Enormous tissue shift and consequential missing correspondences mark a common side effect of tumor resection and pose a major challenge in registering pre- to post-operative

*diana.waldmannstetter@tum.de

images. The same holds true for intra-operative imaging in order to keep track of the surgery progress. A fast and accurate image registration method is crucial for the precise estimation of tumor resection. Recent advances in the field of deep learning also benefited medical image registration. Methods like *VoxelMorph (VM)* [6], *LapIRN* [12], and *TransMorph* [7] have demonstrated that unsupervised deformable image registration is a promising alternative to frameworks based on iterative optimization algorithms like *Advanced Normalization Tools (ANTs)* [3] or *Elastix* [8]. Learnable methods provide comparable performance while significantly improving processing time. Within the scope of the *Brain Tumor Sequence Registration Challenge (BraTS-Reg)* [4], there has also been considerable development of registration algorithms for MRI brain images before and after tumor resection [1, 10, 11, 13, 17, 18]. Unsupervised *Deformable Registration Networks (DRN)* can nicely register healthy brain scans [6, 12, 7]; however, they oftentimes struggle with large pathologies. Therefore, *Instance-Specific Optimization (IO)* proved advantageous to mitigate major deformations [11, 17]. Existing deep learning registration algorithms usually make use of a single similarity metric, oftentimes coupled with a smoothing regularization based on the deformation field, to be optimized in the loss function [6, 12]. However, there is only limited literature addressing the combination of multiple similarity metrics to improve registration results [2, 15, 16, 19].

In this work, we extend an unsupervised *DRN* using a combination of image similarity metrics in the loss function, which are optimized simultaneously. We benchmark the performance of our approach against the baselines on two challenging datasets of pre- to post-operative as well as pre- to intra-operative brain tumor images. Furthermore, we compare our approach to state-of-the-art (SOTA) methods, achieving competitive results. Following [6, 11, 17], we opt for instance-specific optimization in addition to the *DRN*. We demonstrate that the simultaneous optimization of two similarity metrics can improve registration accuracy in terms of *Target Registration Error (TRE)* on expert landmark annotations.

2 Methods

Our workflow consists of three steps. First, we train a *Deformable Registration Networks (DRN)*, followed by *Instance-Specific Optimization (IO)* at test time. Both *DRN* and *IO* optimize the same loss function. We then evaluate the registration performance in terms of *Target Registration Error (TRE)*.

2.1 Unsupervised Deformable Registration

We start our approach with a *DRN*, similar to [6]. Given two 3D images X and Y , where one denotes the source image S and the other one the target image T , the network models the following function $f_{\theta}(X, Y) = u$, where the displacement field u , aligning X and Y , is defined bidirectionally, leading to $u_{s,t} = f_{\theta}(S, T)$ and $u_{t,s} = f_{\theta}(T, S)$ with θ being a set of learning parameters. Image X is then warped

with the displacement field using a spatial transform. While many *Convolutional Neural Network (CNN)*-based models are applicable here, like [6], we opt for a *U-Net*-like architecture with encoder, decoder and skip connections. The loss function comprises two main components, which are an image similarity metric and a smoothness regularizer (first-order gradient’s norm) for the displacement field. In addition to optimizing a single similarity metric as part of the loss function, we opt for optimizing multiple metrics simultaneously. An overview of the workflow is shown in Figure 1.

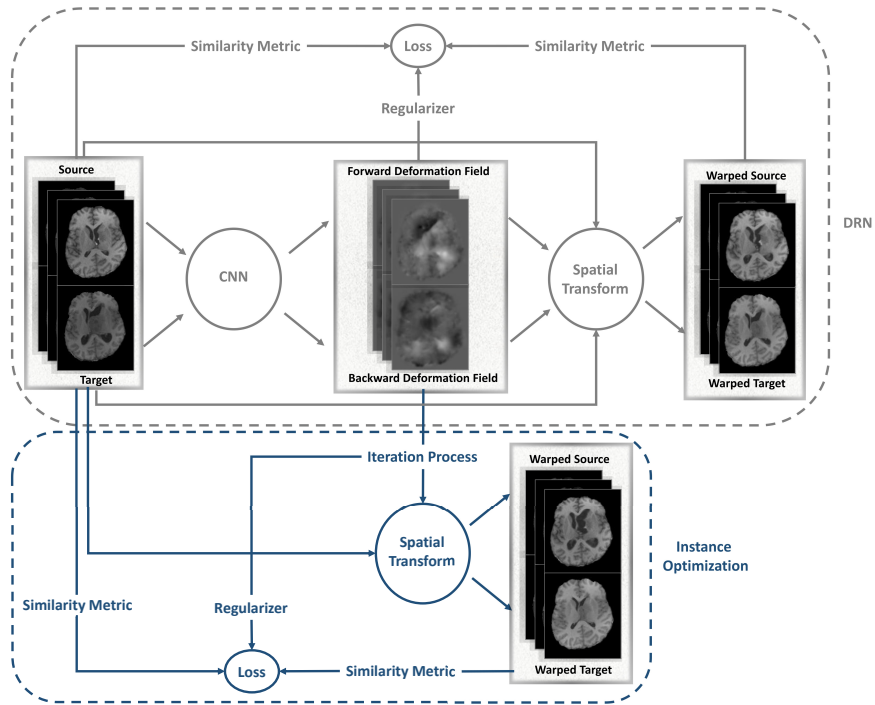


Fig. 1. Overview of the workflow. An unsupervised deformable registration network (*DRN*, top) is combined with *Instance-Specific Optimization (IO)* (bottom) for iterative refinement at test time using the output deformation field of the trained *DRN*. *DRN* as well as *IO* are trained bidirectionally, providing both forward and backward deformation fields. Each loss function is composed of either an individual or a combination of image similarity metrics together with a smoothness regularizer.

2.2 Proposed Combined Loss Function

We define the objective function L for bidirectional training as follows:

$$L = \sum_{n=1}^N \left(L_{Sim_n}^{forward} \cdot \omega_n + L_{Sim_n}^{backward} \cdot \omega_n \right) + L_{Reg} \cdot \lambda \quad (1)$$

where N is the number of similarity metrics L_{Sim} , L_{Reg} is the regularization term, and the respective weights are denoted by ω_n and λ .

2.3 Instance-specific Optimization

Since the registration results of a plain *DRN* might not always be sufficient, especially in the case of pathologies, *IO* is added in order to further refine the registration. Similar to [6], we take the output displacement field of *DRN* as initialization for a gradient descent-based iterative optimization on each test scan individually, following the initial training process. This technique optimizes the same loss function that is used for *DRN*. An overview of the complete method is given in Figure 1.

2.4 Evaluation

We evaluate all experiments by calculating the mean and median *TRE* between the expert landmark annotations and the warped landmarks on the respective test sets. We use the Euclidean distance to calculate the *TRE*, as illustrated in Figure 2.

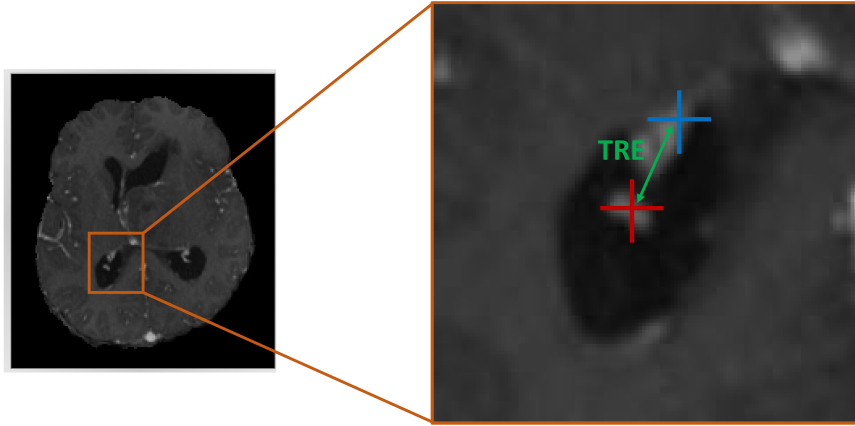


Fig. 2. Evaluation of the *Target Registration Error (TRE)* between expert landmark annotation (red) and warped landmark after image registration (blue). The green arrow indicates the Euclidean distance between the two points.

3 Experiments and Results

We perform experiments using the different loss functions on two brain MRI datasets. Additionally, we implement two *SOTA* methods for comparison.

3.1 Data and Pre-Processing

Training and evaluation are performed on two brain tumor datasets:

Pre-Post-OP (PP): Contains 300 cases of MRI scans of brains with one timepoint before and one timepoint after tumor resection. It is comprised of the official training+validation dataset of *BraTS-Reg* [4] with 160 cases and three datasets collected at *Klinikum rechts der Isar (TUM)* with 49, 30, and 61 cases, respectively.

Pre-Intra-OP (PI): Contains 119 cases of MRI scans of brains with one timepoint before and one timepoint during tumor surgery and originates again from *Klinikum rechts der Isar (TUM)*.

All cases contain either three or four of the MRI sequences native T1-weighted, contrast-enhanced T1, T2-weighted (T2), T2 Fluid Attenuated Inversion Recovery (Flair). For each test set, six landmarks annotated by clinical experts are provided for each case, resulting in a number of 180 landmarks on 30 patients for *PP* and 160 landmarks on 20 patients for *PI*. We pre-process the data using the *BraTS toolkit* [9], which includes re-orientation into the same coordinate system, rigid co-registration to a brain atlas as well as brain extraction. Additionally, intensity normalization is applied to all images.

3.2 Similarity Metrics

We demonstrate the simultaneous optimization strategy on the similarity metrics *Mean Squared Error (MSE)* and *Normalized Cross Correlation (NCC)*, which are widely used in terms of medical image registration tasks [6].

3.3 Training and Testing

We perform multi-channel training for *DRN* and *IO* with the respective available MRI sequences. We split the *PP* dataset into training (80%), validation (10%), and test (10%) and select the model for testing that shows a minimal loss on the validation set. Since we have much fewer cases available for the experiments on the *PI* dataset, we waive the validation set here and decide on a fixed number of 600 training epochs in all experiments. At test time, the *DRN*'s output deformation field serves as input to the 30 iterations of *IO*. For each dataset, we compare the combined loss of $MSE + NCC$ against the individual addends, both for the initial *DRN* training as well as the *IO*. Therefore, we exhaustively explore loss combinations for *DRN* and *IO*, as depicted in Table 1.

The implementation is inspired by [6] using *Pytorch* 1.8.1 [14]. We use learning rates $1e-4$ and $1e-3$ for *DRN* and *IO*, respectively. Image similarity metrics

are weighted equally in the loss function, summing up to 1 for the similarity term. Smoothness regularization weight is set to 1.0 for all experiments for a fair comparison.

3.4 Baselines

Moreover, we compare our approach with a deformable *SyN* registration by *ANTs* [3], and *VM* [6], both using the respective T1-weighted sequences. We implement two variants of *VM* [6], available at [5], that employ *MSE* and *NCC* as respective image similarity metrics. Therefore, we use default learning rate $1e-4$ and recommended smoothness regularization weights of 0.02 and 1.5 for *MSE* and *NCC*, respectively. Likewise, *ANTs SyN* [3] is implemented using default parameters. Since we opt for deformable registration without prior rigid/affine alignment, we apply the same for *VM* and *ANTs SyN*.

3.5 Results

Quantitative results on both datasets can be observed from Table 1. The *TREs* indicate that for *PP*, *DRN* with *NCC* loss achieves the lowest mean error. When coupling *DRN* with *IO*, for all possible combinations, mean *TRE* is always lowest when using *MSE+NCC* during *IO*. On *PI*, for all experiments with *DRN* and *DRN+IO*, mean *TRE* is lowest when combining *MSE* and *NCC* losses.

Table 1. Mean *TRE* in *mm* with standard deviation and for different losses for *DRN* and *DRN+IO* on the Pre-Post-OP and Pre-Intra-OP test sets. Shown are the results on all possible combinations of loss functions. The best results in each category are highlighted. Statistical comparisons are provided in the supplementary materials.

Loss [DRN]	Loss [IO]	Pre-Post-OP	Pre-Intra-OP
MSE	(not applied)	2.40±1.56	3.48±3.45
MSE	MSE	2.21±1.56	3.27±3.46
MSE	NCC	1.81±1.45	3.24±3.39
MSE	MSE+NCC	1.76±1.36	3.17±3.39
NCC	(not applied)	2.18±1.52	3.31±2.68
NCC	MSE	2.06±1.50	2.96±2.78
NCC	NCC	1.80±1.44	2.71±2.79
NCC	MSE+NCC	1.77±1.36	2.68±2.72
MSE+NCC	(not applied)	2.19±1.49	3.07±2.96
MSE+NCC	MSE	2.07±1.48	2.94±3.05
MSE+NCC	NCC	1.80±1.44	2.86±2.95
MSE+NCC	MSE+NCC	1.73±1.34	2.76±2.89

Table 2 shows a comparison of the best *DRN+IO* with results achieved by baseline approaches *VM* and *ANTs*. For *PP*, *DRN+IO* shows lowest mean *TREs*, while for *PI*, this is the case for *ANTs SyN*. Figure 3 shows sample qualitative results on *PP*.

Table 2. Comparison of registration methods. Mean *TRE* in *mm* with standard deviation on the Pre-Post-OP and Pre-Intra-OP datasets for the best *DRN+IO* compared to *VM* and *ANTs SyN*. The proposed method is on par with *SOTA* registration methods.

Method	Pre-Post-OP	Pre-Intra-OP
DRN+IO	1.73±1.34	2.68±2.72
VM (MSE)	2.98±2.11	3.66±2.90
VM (NCC)	2.09±1.54	2.37±2.37
ANTs SyN	2.02±1.49	1.81±1.17

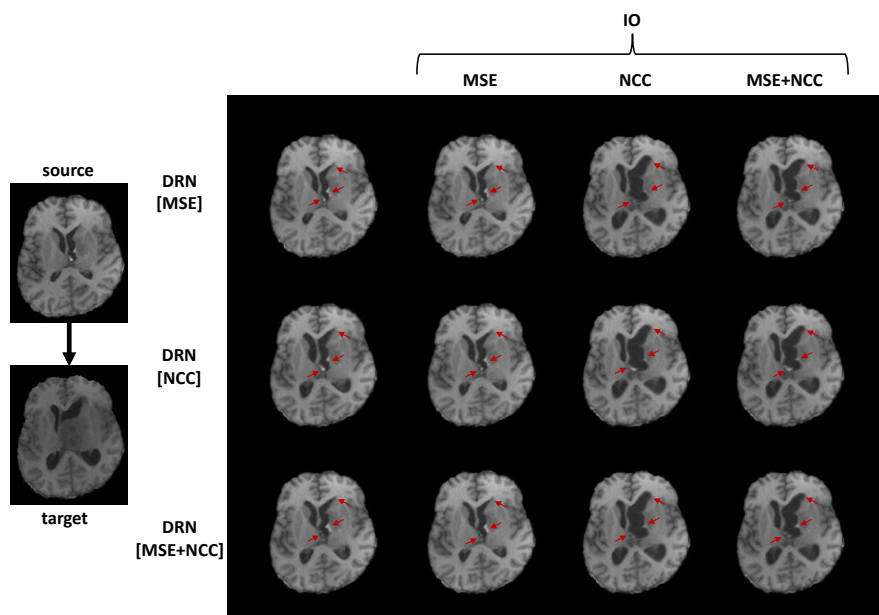


Fig. 3. Sample qualitative results on the Pre-Post-OP data. Differences are marked with red arrows in the registered scans. *NCC* seems to be generally better in aligning the images while preserving anatomical structures than *MSE*. Combining the losses leads to reasonable solutions.

4 Discussion

In Table 1, we observe that combining MSE and NCC losses consistently improves IO performance in both datasets. When applied to DRN only, the combination still performs best for PI while showing comparable results to NCC for PP . Furthermore, Table 2 illustrates our method achieves competitive results compared to $SOTA$ methods. Moreover, for PP , the proposed approach outperforms all baseline methods. For PI , $ANTs SyN$ performs best. A potential explanation might be the rather small training dataset of 99 exams. DRN as well as VM would likely benefit from a bigger training dataset. NCC is generally better than MSE in aligning the source image to the target image while preserving the source’s anatomy. Figure 3 visualizes this for an example.

There are several limitations to this study. The evaluation is performed on rather small test sets of 20 for PI and 30 for PP . The used datasets are fairly specific, so for generalization purposes, an extension toward other registration tasks would be insightful. Even though it could be fine-tuned, we use a fixed weight for regularization on the deformation field in our approach.

5 Conclusion and Future Work

In this work, we propose simultaneously optimizing multiple image similarity metrics for image registration tasks. For demonstration purposes, we combine the well-established metrics MSE and NCC . We evaluate $DRNs$ with and without IO in two challenging multi-modal 3D registration settings, namely pre- to post-operative and pre- to intra-operative glioma MRI . We demonstrate that our proposed optimization strategy, here implemented by means of a simple summation, benefits registration performance with regard to TRE . Moreover, we conduct extensive comparisons against $SOTA$ baselines. Future work should investigate the addition of further similarity metrics such as *Mutual Information*. Besides, introducing different weights for the individual parts of the loss function (instead of equally weighting) might further enhance registration performance.

Acknowledgements

Supported by Deutsche Forschungsgemeinschaft (DFG) through TUM International Graduate School of Science and Engineering (IGSSE), GSC 81. BM, BW and FK are supported through the SFB 824, subproject B12. BM acknowledges support by the Helmut Horten Foundation.

References

1. Abderezaei, J., Pionteck, A., Chopra, A., Kurt, M.: 3d inception-based transmorph: Pre-and post-operative multi-contrast mri registration in brain tumors. arXiv preprint arXiv:2212.04579 (2022)
2. Avants, B.B., Tustison, N.J., Song, G., Cook, P.A., Klein, A., Gee, J.C.: A reproducible evaluation of ants similarity metric performance in brain image registration. *Neuroimage* **54**(3), 2033–2044 (2011)
3. Avants, B.B., Tustison, N., Song, G., et al.: Advanced normalization tools (ants). *Insight j* **2**(365), 1–35 (2009)
4. Baheti, B., Waldmannstetter, D., Chakrabarty, S., Akbari, H., Bilello, M., Wiestler, B., Schwarting, J., Calabrese, E., Rudie, J., Abidi, S., et al.: The brain tumor sequence registration challenge: establishing correspondence between pre-operative and follow-up mri scans of diffuse glioma patients. arXiv preprint arXiv:2112.06979 (2021)
5. Balakrishnan, G., Zhao, A., Sabuncu, M., Guttag, J., Dalca, A.V.: voxelmorph: Learning-based image registration, <https://github.com/voxelmorph/voxelmorph>, accessed: 25.02.2023
6. Balakrishnan, G., Zhao, A., Sabuncu, M.R., Guttag, J., Dalca, A.V.: Voxelmorph: a learning framework for deformable medical image registration. *IEEE transactions on medical imaging* **38**(8), 1788–1800 (2019)
7. Chen, J., Frey, E.C., He, Y., Segars, W.P., Li, Y., Du, Y.: Transmorph: Transformer for unsupervised medical image registration. *Medical image analysis* **82**, 102615 (2022)
8. Klein, S., Staring, M., Murphy, K., Viergever, M.A., Pluim, J.P.: Elastix: a toolbox for intensity-based medical image registration. *IEEE transactions on medical imaging* **29**(1), 196–205 (2009)
9. Kofler, F., Berger, C., Waldmannstetter, D., Lipkova, J., Ezhov, I., Tetteh, G., Kirschke, J., Zimmer, C., Wiestler, B., Menze, B.H.: Brats toolkit: translating brats brain tumor segmentation algorithms into clinical and scientific practice. *Frontiers in neuroscience* p. 125 (2020)
10. Meng, M., Bi, L., Feng, D., Kim, J.: Brain tumor sequence registration with non-iterative coarse-to-fine networks and dual deep supervision. arXiv preprint arXiv:2211.07876 (2022)
11. Mok, T.C., Chung, A.: Robust image registration with absent correspondences in pre-operative and follow-up brain mri scans of diffuse glioma patients. arXiv preprint arXiv:2210.11045 (2022)
12. Mok, T.C., Chung, A.C.: Large deformation diffeomorphic image registration with laplacian pyramid networks. In: *Medical Image Computing and Computer Assisted Intervention–MICCAI 2020: 23rd International Conference, Lima, Peru, October 4–8, 2020, Proceedings, Part III* 23. pp. 211–221. Springer (2020)
13. Mok, T.C., Chung, A.C.: Unsupervised deformable image registration with absent correspondences in pre-operative and post-recurrence brain tumor mri scans. In: *Medical Image Computing and Computer Assisted Intervention–MICCAI 2022: 25th International Conference, Singapore, September 18–22, 2022, Proceedings, Part VI*. pp. 25–35. Springer (2022)
14. Paszke, A., Gross, S., Massa, F., Lerer, A., Bradbury, J., Chanan, G., Killeen, T., Lin, Z., Gimelshein, N., Antiga, L., Desmaison, A., Kopf, A., Yang, E., DeVito, Z., Raison, M., Tejani, A., Chilamkurthy, S., Steiner, B., Fang, L., Bai, J., Chintala, S.: PyTorch: An Imperative Style, High-Performance Deep Learning Library. In:

- Wallach, H., Larochelle, H., Beygelzimer, A., d'Alché Buc, F., Fox, E., Garnett, R. (eds.) *Advances in Neural Information Processing Systems* 32. pp. 8024–8035. Curran Associates, Inc. (2019), <http://papers.neurips.cc/paper/9015-pytorch-an-imperative-style-high-performance-deep-learning-library.pdf>
15. Uss, M.L., Vozel, B., Abramov, S.K., Chehdi, K.: Selection of a similarity measure combination for a wide range of multimodal image registration cases. *IEEE Transactions on Geoscience and Remote Sensing* **59**(1), 60–75 (2020)
 16. Wachs, J., Stern, H., Burks, T., Alchanatis, V.: Multi-modal registration using a combined similarity measure. *Applications of Soft Computing* **52**, 159–168 (2009)
 17. Wodzinski, M., Jurgas, A., Marini, N., Atzori, M., Muller, H.: Unsupervised method for intra-patient registration of brain magnetic resonance images based on objective function weighting by inverse consistency: Contribution to the brats-reg challenge. *arXiv preprint arXiv:2211.07386* (2022)
 18. Zeineldin, R.A., Karar, M.E., Mathis-Ullrich, F., Burgert, O.: Self-supervised ireg-net for the registration of longitudinal brain mri of diffuse glioma patients. *arXiv preprint arXiv:2211.11025* (2022)
 19. Zhou, J., Liu, Q.: A combined similarity measure for multimodal image registration. In: 2015 IEEE International Conference on Imaging Systems and Techniques (IST). pp. 1–5. IEEE (2015)

Appendix

Table 3. *P-values* and *95% Confidence Intervals (CI)* of *Paired Samples T-Tests* on the *TREs* of competitive methods for the Pre-Post-OP and the Pre-Intra-OP datasets. Methods are given by declaring the used losses for the *Deformable Registration Network (DRN)* and the *Instance Optimization (IO)*, respectively. Registration results improve significantly in two cases, when using the combination of two losses.

Method 1	Method 2	p-value [CI] (Pre-Post-OP)	p-value [CI] (Pre-Intra-OP)
DRN (NCC)	DRN (MSE+NCC)	0.85 [-0.09; 0.07]	0.05 [0.00; 0.47]
DRN (MSE) + IO (NCC)	DRN (MSE) + IO (MSE+NCC)	0.13 [-0.01; 0.10]	0.23 [-0.04; 0.16]
DRN (NCC) + IO (NCC)	DRN (NCC) + IO (MSE+NCC)	0.22 [-0.02; 0.08]	0.50 [-0.06; 0.13]
DRN (MSE+NCC) + IO (NCC)	DRN (MSE+NCC) + IO (MSE+NCC)	0.03 [0.01; 0.13]	0.03 [0.01; 0.19]

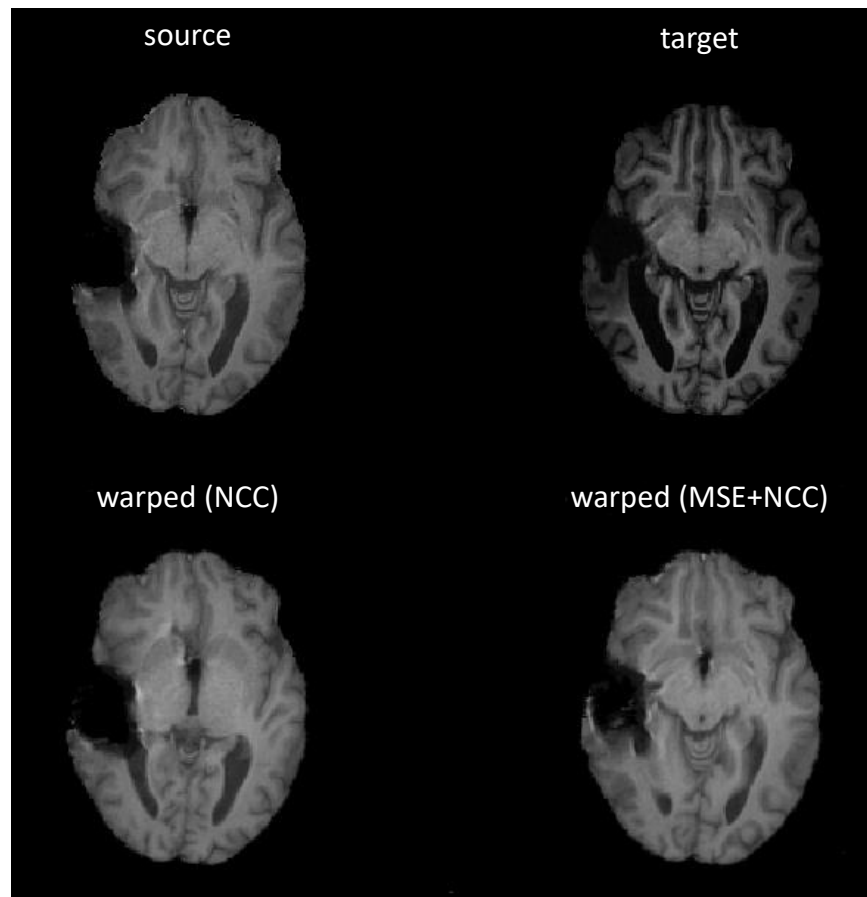


Fig. 4. Sample registration results on the Pre-Intra-OP dataset. Registration with combined losses $MSE+NCC$ shows improved registration in comparison to registration with NCC only, especially nearby the tumor and the resection cavity, respectively.